Adsorption and Diffusion of Si Adatom on Hydrogenated Si(100) Surfaces

Sukmin Jeong and Atsushi Oshiyama
Institute of Physics, University of Tsukuba, Tennodai, Tsukuba 305, Japan

(Received 6 June 1997)

We present first-principles total-energy calculations which provide a detailed picture of adsorption and diffusion of a Si adatom on hydrogenated Si(100) surfaces. We find that the adatom spontaneously substitutes for the H atom upon adsorption. We also find that the pathways and barriers of the adatom diffusion are sensitive to H coverage. Calculated results are consistent with H-induced variation in morphology of overlayers observed in epitaxial growth. [S0031-9007(97)04619-X]

PACS numbers: 68.35.Fx, 68.35.Bs, 68.55.–a, 81.10.Aj

Morphology of thin films is in general determined by energetics and kinetics of atomic reactions during epitaxial growth. Introducing foreign atoms that may change the balance between the two onto the crystal growth front could thus lead to remarkable change in morphology of the overlayers (surfactant effects) [1]. Hydrogen in homo- and heteroepitaxy on Si(100) surfaces is such an example that is important both scientifically and technologically [2–9]. In chemical vapor deposition and gas-source molecular beam epitaxy (MBE), the growth front is terminated by H. Morphology of Si overlayers indeed depends on H coverage [8]. In solid source MBE, H is introduced intentionally to assist in epitaxial growth. For instance, Ge grows layer by layer on Si(100) using H as a surfactant [7]. Even at an initial stage of homoepitaxy, H causes changes in shape and density of two-dimensional Si islands [9].

Structures of H-terminated Si(100) have been well identified [2]: three distinctive structures (2×1, 3×1, and 1×1) appear with increasing H dose or H chemical potential [10]; the 2×1 is a monohydride phase in which the H atoms saturate the dangling bonds of the Si dimers on the clean surface; the 1×1 is a dihydride phase in which the dimers are broken and the dangling bonds are saturated [11]; the 3×1 is an ordered mixture of the monohydride and the dihydride units. Little is known, however, about microscopic processes, adsorption and diffusion processes of an adatom, which lead to the change in morphology of the overlayers.

In this Letter, we present total-energy electronic-structure calculations within the local density approximation (LDA), which provide a detailed picture of the adsorption and diffusion mechanisms of a Si adatom on the hydrogenated Si(100) surface. We find that the adatom *substitutes for hydrogen* upon adsorption. Activation energies for the substitutional adsorption is *absent*. We also find that the mechanism and the activation energy of the adatom diffusion are *sensitive* to H coverage Θ_H: isotropic diffusion with the activation energy of 1 eV for $\Theta_H \ll 1$, complex diffusion combined with capture and release of H atoms for monohydride phase ($\Theta_H = 1$), and drastic increase in activation energy for the dihydride phase ($\Theta_H = 2$). The obtained results are rich and in sharp contrast with those for the clean Si(100).

All calculations have been performed by use of norm-conserving pseudopotentials [12], LDA [13] for exchange correlation energy, and conjugate-gradient minimization technique as reported elsewhere [14]. The surface is simulated by a repeating slab model in which five Si atomic layers and the 8.76 Å vacuum region are included. The bottom of the slab has a bulklike structure with each Si saturated by two H atoms. On the top of the slab, which simulates the real surface, a H adlayer plus a Si adatom is considered. We find that the $p(\sqrt{8} \times \sqrt{8})R45^\circ$ periodic cell in the lateral directions, the four k-points in surface Brillouin zone, and the 8-Ry cutoff energy in the plane wave basis set are necessary to obtain converged results [15]. We use a local potential for H, while s and p nonlocality is taken into account for Si. The geometry optimization has been performed for all atoms except for the bottom-most H and Si atoms. In the optimized geometries the remaining forces acting on the atoms are less than 0.005 Ry/Å. We have carried out the calculation for the 2×1 monohydride, and the 1×1 dihydride Si(100)-H surface. The obtained structural parameters as well as the relative stability of the two phases as a function of the H chemical potential are in good agreement with the previous results [10].

We set out adsorption of a Si adatom on the 2×1 monohydride surface. Figure 1 shows the stablest adsorption geometry for the adatom. The geometry possesses no symmetry at all, and the adsorption energy is calculated to

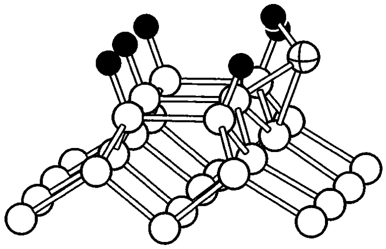

FIG. 1. Stablest geometry of a Si adatom on the 2×1 monohydride Si(100). Crossed, black, and open circles denote a Si adatom, H atoms, and Si atoms, respectively.

be 3.2 eV. A striking feature of the geometry is the substitutional adsorption: The Si adatom forms a bond with a substrate Si atom (bond length: 2.26 Å) which releases a H atom, and the H atom is in turn bonded to the adatom. The adatom also forms a weak bond (bond length: 2.57 Å) with a subsurface Si atom and is thus stabilized.

In order to obtain activation energies for the substitutional adsorption, we have computed total energies for several fixed vertical distances, $z_{\text{Si-Si}}$, between the adatom and the substrate. Figure 2 shows the total energy as a function of the H-substrate distance z with the fixed $z_{\text{Si-Si}} = 3.5$ Å. The H atom is released from the Si dimer atom and is bonded to the Si adatom. The energy barrier to break the bond between the H and the Si dimer atom is *absent*. This infers that the Si adatom spontaneously substitutes for the H atom upon adsorption. When the adatom is located far from the substrate, there are at least two (meta)stable geometries in which the H atom is bonded either to the substrate Si atom or to the Si adatom. Figure 2 also presents such a case with $z_{\text{Si-Si}} = 5.5$ Å. There is an energy barrier between the two geometries. When the adatom becomes close to the substrate, the barrier remains to exist in usual cases. In the present case, however, the small radius of H allows the adatom to approach the substrate so close that the adatom forms weak floating bonds with the substrate Si atoms as well as with the H atom. This reduces, or may compensate completely for, the energy barrier required for the simple bond breaking between the substrate Si and H atoms.

The substitutional adsorption with no activation energy occurs at many sites. Figure 3 is the calculated total-energy surface for the Si adatom on the monohydride Si(100). In obtaining this total-energy surface, we first fix the Si adatom at a site in the lateral plane, and then relax all the surrounding atoms and also the adatom itself in the vertical direction. We repeat these total-energy calculations for 15 sites spaced 0.96 Å apart in an irreducible quarter of the $p(2 \times 1)$ lateral cell (Fig. 3), and then interpolate the calculated values with 15 irreducible plane waves to obtain global features of the total-energy surface. The substitutional adsorption takes place when the adatom approaches the surface along with being close enough to the H atom (Fig. 3).

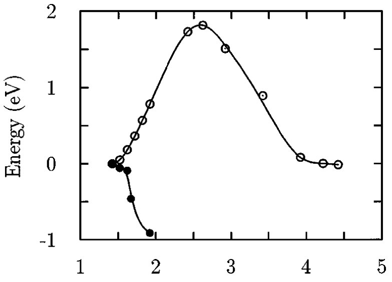

FIG. 2. Total energies as a function of the distance between the H and the topmost Si atom z for fixed distances between the Si adatom and the topmost Si atom $z_{\text{Si-Si}}$. Black and open circles show the calculated values for $z_{\text{Si-Si}} = 3.5$ and 5.5 Å, respectively.

Figure 3 also provides important information on the diffusion of the Si adatom on the monohydride Si(100). The diffusion pathway perpendicular to the substrate dimer rows is a motion along *ADAEA*... passing through a saddle point near *D*. We find that release and capture of the H atom is an important process in the adatom diffusion: The adatom is at first adsorbed substitutionally at the stablest site *A*, migrates to the site *D* with the H atom, then releases the H atom to overcome the saddle point, and proceeds to the next stablest site *A* with capturing another H atom. The rate determining process is the H release and the diffusion barrier is about 1 eV. The diffusion parallel to the substrate dimer rows is also combined with the release and capture of H atoms. The exchange process in which the subsurface Si atom forming a dimer is replaced by the adatom and then migrates is also involved in the diffusion. Detailed atomic processes in the diffusion will be reported elsewhere. We here just report the diffusion pathway as *ABACEA* ... and the diffusion barrier is about 0.7 eV. The H release is again an essential process which determines the diffusion barrier. We emphasize that the diffusion mechanism is quite different from that on the clean surface [16].

To relate the present calculation with the experiments, the adatom diffusion for lower H coverage Θ_{H} is of high interest. Using scanning tunneling microscopy and kinetic simulations with an assumption of the anisotropic diffusion barrier, Vasek *et al.* [9] have deduced the activation energy of the adatom along the dimer rows: 1.34 eV for $\Theta_{\text{H}} = 0.04$, and 1.44 eV for $\Theta_{\text{H}} = 0.08$. These values are substantially larger than the activation energy on the clean surface ($Q_{\parallel} = 0.6$ eV and $Q_{\perp} = 1.0$ eV) [16,17]. We have thus performed the LDA calculations for $\Theta_{\text{H}} = 0.25$ using the $p(\sqrt{8} \times \sqrt{8})R45^\circ$ lateral cell. We have not explored a complete total-energy surface. Instead we have searched diffusion pathways along the dimer rows by fixing only the x coordinate (Fig. 4) of the adatom, minimizing the total energy with the constraint, and repeating the minimization for more than ten different x coordinates of the adatom. It is found that there are three distinctive pathways along which the activation energies are 1.0–1.7 eV (Fig. 4). Along any pathway, the stablest site for the adatom is *M* in Fig. 4 which is the stablest site in the case of the clean surface, and the saddle point is in the vicinity of the H atom. A hydrogenated dimer works as a blockade for the adatom diffusion along the dimer rows. For lower Θ_{H} the diffusion along the dimer rows may take place along a detour which includes the path perpendicular to the dimer rows (Fig. 4). In this case the activation energy is 1 eV [16].

The obtained result that the diffusion is less anisotropic compared with that on the clean surface is consistent with the observation of less anisotropic two-dimensional islands [9]. The finding that the hydrogenated dimer is

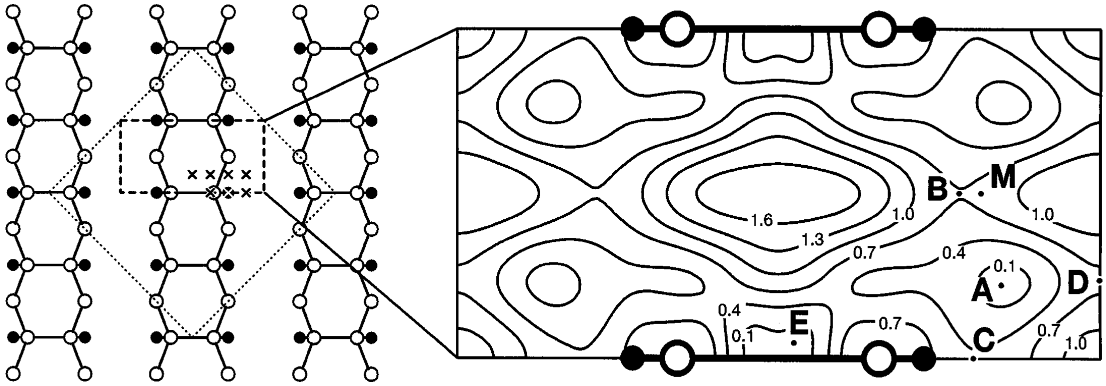

FIG. 3. Calculated total-energy surface for a Si adatom on the 2 × 1 monohydride Si(100) surface (Si: open circle; H: black circle). The first contour represents the energy line of 0.1 eV with respect to the most stable adsorption site (*A*) and the subsequent contour spacing is 0.3 eV. In the left part, the $p(2 \times 1)$ unit cell, in which the energy surface is shown, is indicated by the dashed line and the $p(\sqrt{8} \times \sqrt{8})R45^\circ$ unit cell, in which the calculations have been performed, by the dotted line. The substitutional adsorption of the adatom without activation energies takes place, at least, on seven sites marked by crosses in the left panel. Sites *A* and *E* are (meta)stable adsorption sites. The total energies above the dimer (around *E*) correspond to those in the substitutional geometries even though there are energy barriers for the substitution.

a blockade also explains the increase in island number density under H exposure [9]. With random distribution of the hydrogenated dimers, diffusion of the adatom is suppressed as in a percolation system. This causes the decrease in size and increase in number of the two-dimensional islands.

The reasons for the spontaneous substitutional adsorption are the small atomic radius of H and the strong covalency of group IV atoms. We therefore expect that the substitutional adsorption of the adatom occurs also in heteroepitaxy of Ge on the Si(100)-H. In that case the crystal growth front is always terminated by H. Group V atoms which are known to work as surfactants in heteroepitaxial growth of Ge on the Si(100) also terminate the growth front [18]. The substitutional adsorption that we have found here is thus expected to be important for the surfactant effect of H in the heteroepitaxy [7]. Direct experimental evidence for the spontaneous substitutional adsorption of the adatom is awaited.

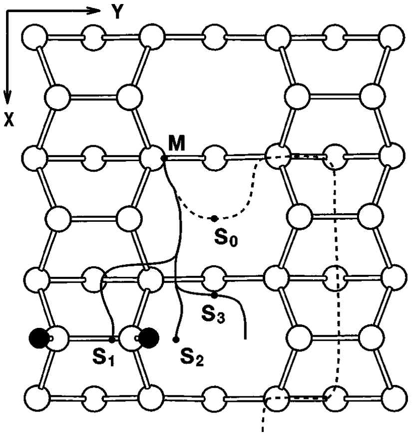

FIG. 4. Top view of diffusion pathways for the Si adatom on the hydrogenated Si(100) with H coverage of $\Theta_H = 0.25$. The stablest site is labeled by *M*, and the saddle points along the pathways by S_1, S_2, and S_3. The saddle point along the detour (dashed line) is labeled by S_0.

With increasing H coverage the 1 × 1 dihydride phase in which the surface SiH_2 units are canted appears. Figure 5 shows the stablest adsorption geometry for the adatom. Again the substitutional adsorption takes place without the energy barrier. The bond lengths and angles around the adatom in the resulting stablest geometry are strikingly bulklike. As a result of this, the calculated adsorption energy is 5.3 eV much larger than the monohydride case.

Figure 6 is the calculated total-energy surface for the Si adatom on the dihydride Si(100). This has been obtained with the same procedure as for the monohydride case. Diffusion pathways of the Si adatom are *XYXY*... or *XSXS*... in Fig. 6. We find that the diffusion is isotropic and the activation energy increases remarkably: 2.7 eV for both pathways. This increase in the diffusion barrier is due to the high stability of the stablest geometry, and the isotropic energy barrier due to a common geometric feature (i.e., two dangling bonds) in the two saddle point geometries *Y* and *S*.

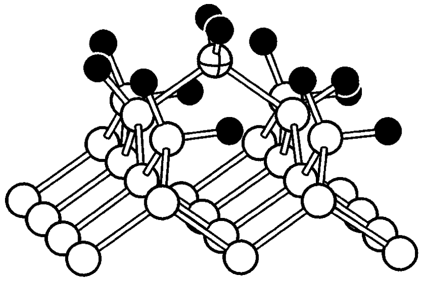

FIG. 5. Stablest geometry of a Si adatom on the 1 × 1 canted dihydride Si(100). Crossed, black, and open circles denote a Si adatom, H atoms, and Si atoms, respectively.

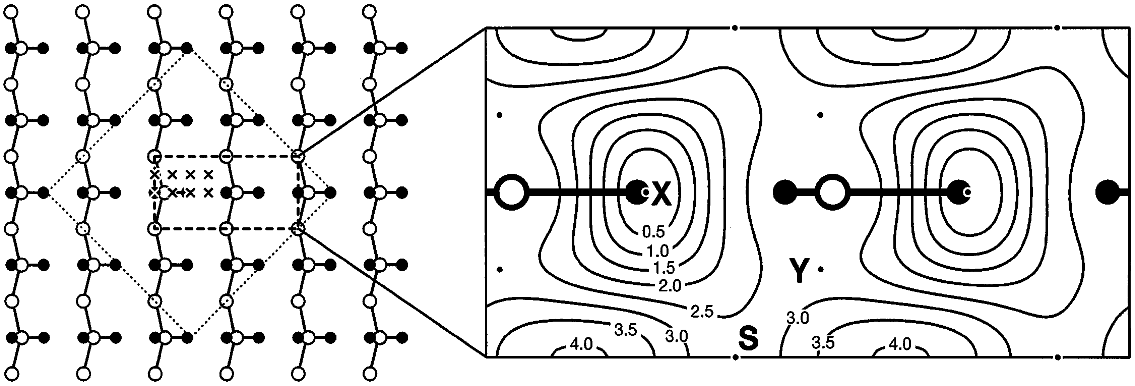

FIG. 6. Calculated total-energy surface for an Si adatom on the 1 × 1 dihydride Si(100) surface (Si: open circle; H: black circle). The first contour represents the energy line of 0.5 eV with respect to the most stable adsorption site (*X*) and the subsequent contour spacing is 0.5 eV. The substitutional adsorption of the adatom without activation energies takes place, at least, on eight sites marked by crosses in the left panel. The site *X* is a stable adsorption site, and *S* and *Y* are saddle points for the adatom diffusion.

At the H coverage between the 2 × 1 ($\Theta_H = 1$) and the 1 × 1 ($\Theta_H = 2$) phases, dihydride and monohydride units are likely to coexist. The present results provide a microscopic picture on the Si adatom diffusion on the surface: The adatom is preferentially adsorbed near the dihydride units since the adsorption energy is larger there. Then the diffusion of the adatom is highly suppressed. Alternatively, for the adatom adsorbed in the monohydride region, the dihydride region is a barrier for the diffusion. Copel and Tromp [8] have found that epitaxial growth becomes eventually disrupted when the H coverage exceeds $\Theta_H = 1$ in Si(100) homoepitaxy. We argue that this observation is due to the high diffusion barrier near the dihydride units which we have found in the present calculations.

To conclude, we have presented the LDA calculations which provide a detailed picture of adsorption and diffusion of a Si adatom on hydrogenated Si(100) surfaces. The calculated results offer a firm theoretical framework for understanding microscopic mechanisms of epitaxial growth on the Si(100)-H.

This work was supported in part by Japan Society for the Promotion of Science under Contract No. RFTF96P00203.

[1] M. Copel, M.C. Reuter, E. Kaxiras, and R.M. Tromp, Phys. Rev. Lett. **63**, 632 (1989).
[2] J.J. Boland, Adv. Phys. **42**, 129 (1993), and references therein.
[3] M. Copel and R.M. Tromp, Appl. Phys. Lett. **53**, 2648 (1991).
[4] K. Sumitomo *et al.*, Phys. Rev. Lett. **66**, 1193 (1991).
[5] D.J. Eaglesham, F.C. Unterwald, and D.C. Jacobson, Phys. Rev. Lett. **70**, 966 (1993).
[6] M.J. Bronikowski, Y. Wang, and R.J. Hammers, Phys. Rev. B **48**, 12 361 (1993).
[7] A. Sakai and T. Tatsumi, Appl. Phys. Lett. **64**, 52 (1994).
[8] M. Copel and R.M. Tromp, Phys. Rev. Lett. **72**, 1236 (1994).
[9] J.E. Vasek, Z. Zhang, C.T. Salling, and M.G. Lagally, Phys. Rev. B **51**, 17 207 (1995).
[10] J.E. Northrup, Phys. Rev. B **44**, 1419 (1991).
[11] The 1 × 1 phase is disordered to some extent and the existence of trihydride units is proposed; A. Vittadini, A. Selloni, R. Car, and M. Casarin, Phys. Rev. B **46**, 4348 (1992).
[12] N. Troullier and J.L. Martins, Phys. Rev. B **43**, 1993 (1991).
[13] D.M. Ceperley and B.J. Alder, Phys. Rev. Lett. **45**, 566 (1980).
[14] O. Sugino and A. Oshiyama, Phys. Rev. Lett. **68**, 1858 (1992); M. Saito, O. Sugino, and A. Oshiyama, Phys. Rev. B **46**, 2606 (1992); B.D. Yu and A. Oshiyama, Phys. Rev. Lett. **71**, 585 (1993).
[15] The convergence of the cutoff energy is examined by performing the calculations with 8-Ry, 10-Ry, and 12-Ry cutoff energies. The total-energy differences between the stablest (*A* in Fig. 3) and the saddle-point (*B* in Fig. 3) geometries on the 2 × 1 hydrogenated surface are 0.662 eV (8 Ry), 0.659 eV (10 Ry), and 0.668 eV (12 Ry), respectively. We have also examined the supercell size in lateral directions. The total-energy difference explained above is 0.669 eV with the larger 4 × 4 lateral cell using 8-Ry cutoff energy.
[16] G. Brocks, P.J. Kelly, and R. Car, Phys. Rev. Lett. **66**, 1729 (1991).
[17] Y.W. Mo, J. Kleiner, M.B. Webb, and M.G. Lagally, Phys. Rev. Lett. **66**, 1998 (1991).
[18] B.D. Yu and A. Oshiyama, Phys. Rev. Lett. **72**, 3190 (1994).